Article

Nicotinic acetylcholine receptors regulate growth hormone in pituitary somatotrophs of tigers

Check for updates

Lulu Liu[1], Shilong Yang[2], Longhui Chai[2], Shipei Zhang[2], Dan Liu[3], Haitao Xu[3], Yue Zhao[2], Shiyu Chen [2]✉, Guangshun Jiang [2]✉ & Bin Li [1]✉

The Felidae exhibits remarkable diversity in body size, with lengths ranging from 50 to 370 cm and weights from 1.1 to 423 kg. However, the underlying mechanisms driving this variation remain poorly understood. Here, we focused on the Siberian tiger (*Panthera tigris altaica*), the largest of the six extant tiger subspecies, and revealed the surprising expression of nicotinic acetylcholine receptors (nAChRs) in pituitary somatotrophs, which are crucial for regulating growth hormone (GH) secretion. Single-nucleus RNA sequencing of Siberian tiger pituitary cells exhibited the coexpression of *CHRNA3*, *CHRNB4*, and *CHRNA5* genes in somatotrophs, a finding confirmed by electrophysiological experiments demonstrating the formation of functional nAChRs. Activation of these receptors elevated intracellular Ca^{2+} levels, thereby enhancing GH secretion in somatotrophs. Notably, nAChRs were absent in the pituitary glands of mice, domestic cats, and rats, both in early life and adulthood, despite high acetylcholine levels during early life. These results suggest that nAChRs in Siberian tiger somatotrophs play a pivotal role in GH release, offering new insights into the molecular mechanisms regulating body size in these terrestrial giants.

Terrestrial mammals exhibit an exceptionally wide range of body size, which strongly correlates with life history traits and population dynamics cross the spectrum from mouse to elephant[1,2]. Additionally, mammalian body size adapts to ecological niches through evolutionary processes, influencing intraspecific competition, habitat selection, metabolic rate, and resource use[3–5]. The Felidae, one of the most threatened groups of terrestrial mammals due to habitat loss and hunting, exhibits significant diversity in body size[6–8]. For instance, the smallest member, the Rusty-spotted cat (*Prionailurus rubiginosus*) from the Indian subcontinent and Sri Lanka, measures 50 to 78 cm in length and weighs between 1.1 and 1.6 kg[9]. The largest, the Siberian tiger (*Panthera tigris altaica*), inhabits northeastern China and the frigid forests of Primorye and Khabarovsk in far-eastern Russia, with body lengths ranging from 2.4 to 3.7 meters and weights from 168 to 423 kg[10,11]. The wide variety in body size within the Felidae offers a unique opportunity to investigate the mechanisms underlying the development of these large mammals. In this study, we focus on the Siberian tiger, an apex predator listed as endangered, to explore the molecular basis underlying body size regulation in large Felidae species.

Mammalian body growth is regulated by a complex network of signaling molecules within the endocrine (GHRH/somatostatin-GH-IGF) axis[12–14]. This regulation occurs via two primary mechanisms: a short feedback loop involving growth hormone (GH) stimulators (growth hormone-releasing hormone) and inhibitors (somatostatin) in the hypothalamus[15,16], and a long feedback loop primarily in the liver, where growth hormone stimulates the secretion of insulin-like growth factor 1 (IGF-1)[17–19]. GH acts as a crucial connecting link within this axis, regulating body size development, tissue repair, and metabolism through secretion by pituitary somatotrophs[20,21]. We therefore hypothesize a species-specific mechanism regulating GH release in the Siberian tiger pituitary gland. In this study, we performed single-nucleus RNA sequencing on a Siberian tiger pituitary gland and identified species-specific expression of nicotinic acetylcholine receptors (nAChRs) in somatotrophs. Functional assays indicate that nAChR activation enhances GH secretion in somatotrophs, offering mechanistic insights into body size regulation in Siberian tiger.

Results

Transcriptional clustering of cell populations in Siberian tiger pituitary gland

We established single-nucleus RNA libraries for the pituitary gland of a Siberian tiger using 10× Genomics, detecting 11,313 nuclei and 23,583

[1]College of Chemistry, Chemical Engineering and Resource Utilization, Northeast Forestry University, Harbin, China. [2]College of Wildlife and Protected Area, Northeast Forestry University, Harbin, China. [3]Siberian Tiger Park, Harbin, Heilongjiang, China. ✉e-mail: chenshiyu180236@163.com; jgshun@126.com; libinzh62@163.com

genes, with an average of 7299 UMI transcripts and 2881 genes per nucleus (Supplementary Figs. 1a and 1b). UMI counts indicated no significant difference between the cell clusters of the pituitary gland (Supplementary Fig. 1c). Single-nucleus RNA sequencing data were clustered using Seurat's

shared nearest neighbor (SNN) method and visualized using t-distributed Stochastic Neighbor Embedding (t-SNE) (Fig. 1a). The distinct cell clusters in the pituitary gland (Supplementary Table 2) were annotated based on differential expression of marker genes (Fig. 1b). Five main hormone-
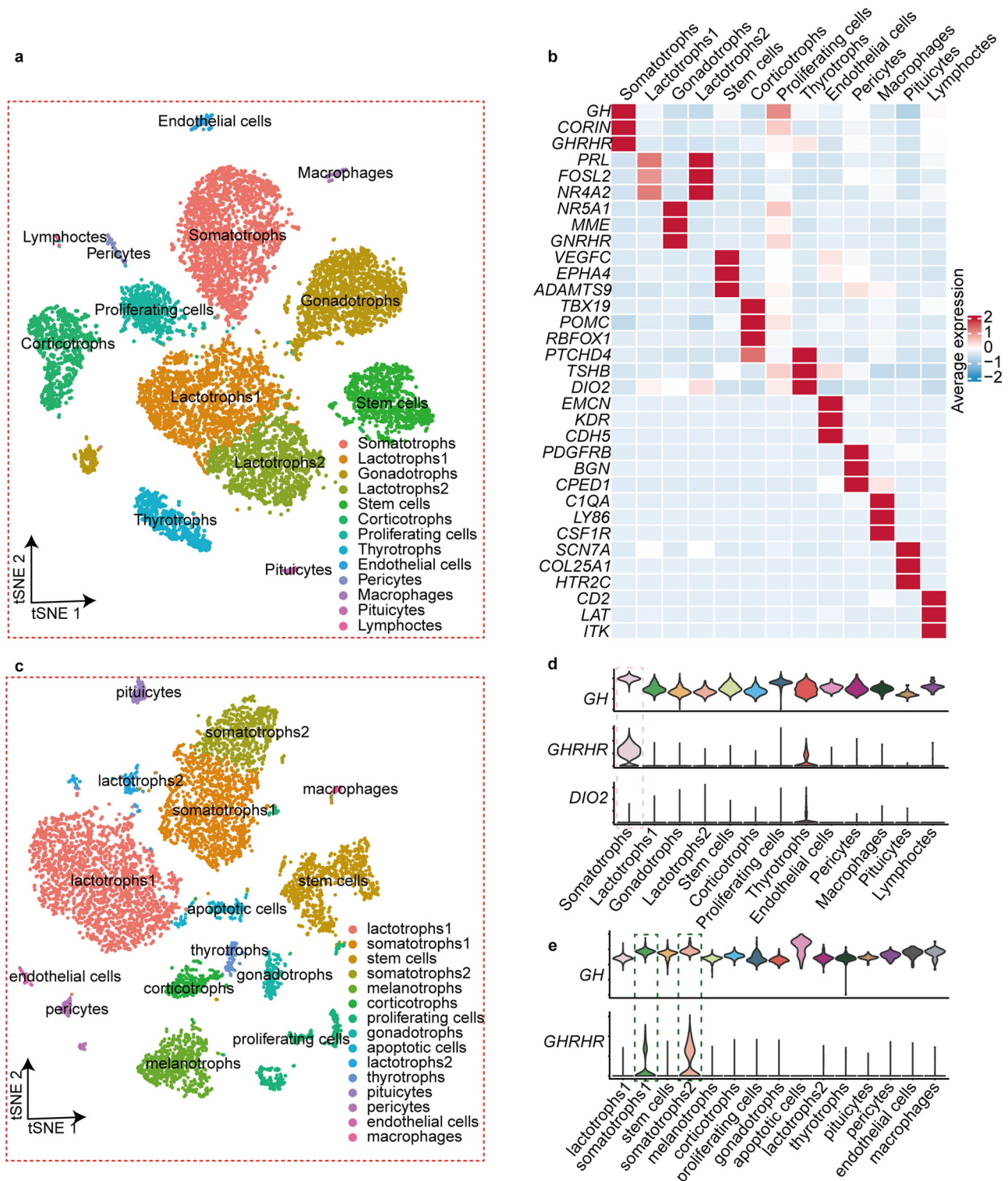

Fig. 1 | Identification of cell types for pituitary gland Sn-RNA-Seq atlases of Siberian tiger and mouse. a t-SNE plot showing single-nucleus atlas of Siberian tiger pituitary gland. Plot (lower right panel) showing indicated cell types. **b** Heatmap of Siberian tiger pituitary gland showing expression of the marker genes in different cell types. **c** t-SNE plot showing single-cell atlas of mouse pituitary gland. Plot (lower right panel) showing indicated cell types. **d** Violin plots showing

expression level of the marker genes *GHRHR* and *GH* within somatotrophs of pituitary in Siberian tiger. *DIO2*, the marker for thyrotrophs, were used to validate the accuracy of thyrotrophs and samototrophs classification. **e** Violin plots showing expression level of the marker genes *GHRHR* and *GH* within somatotrophs of pituitary in mouse.

producing cell types were identified by marker gene expression (Supplementary Fig. 2): somatotrophs (*GH, CORIN, GHRHR*); lactotrophs 1 and 2 (*PRL, FOSL2, NR4A2*); gonadotrophs (*NR5A1, MME, GNRHR*); corticotrophs (*TBX19, POMC, RBFOX1*); and thyrotrophs (*PTCHD4, TSHB, DIO2*) (Fig. 1b). Additionally, we identified stem cells (enriched for *VEGFC, EPHA4*, and *ADAMTS9*), proliferating cells, endothelial cells (*EMCN, KDR, CDH5*), pericytes (*PDGFRB, BGN, CPED1*), macrophages (*C1QA, LY86, CSF1R*), pituicytes (*SCN7A, COL25A1, HTR2C*), and lymphocytes (*CD2, LAT, ITK*). Single-nucleus data from the pituitary gland of mouse[22] were used as reference atlas (Fig. 1c). As expected, all cell types found in the Siberian tiger pituitary gland were also identified in the mouse. These results suggest that the fundamental functions of the Siberian tiger pituitary gland are comparable to those in other mammals.

Nicotinic acetylcholine receptors encoded genes in Siberian tiger somatotrophs

Given that pituitary somatotrophs are crucial for regulating body size growth[23], we compared the expression pattern of somatotrophs between the Siberian tiger and mouse[22] (Fig. 1d, e) by independently extracting matrix data of somatotrophs. After removing batch effects, intergroup differences were analyzed using the FindMarkers function, with ident.1 and ident.2 corresponding to the somatotrophs of the Siberian tiger and mouse, respectively. Interestingly, we found that subunit genes encoding nAChRs[24], including *CHRNA3* (encoding α3), *CHRNB4* (β4), and *CHRNA5* (α5), were expressed in the somatotrophs of the Siberian tiger but not in those of the mouse (Fig. 2a, b). To investigate whether the coexpression of *CHRNA3, CHRNB4*, and *CHRNA5* genes is common in the pituitary glands of terrestrial mammals, we conducted PCR (polymerase chain reaction) to test the expression level of these genes in the pituitary gland of the adult Siberian tiger, as well as in both adult and juvenile domestic cats (*Felis catus*), mice (*Mus musculus*) and rats (*Rattus norvegicus*). Unlike the Siberian tiger, these three subunit genes were absent in the pituitary glands of the cats, mice, and rats (Fig. 2c). Consistently, at the protein level, α5 encoded by *CHRNA5* was detectable in the pituitary gland of the adult Siberian tiger but absent in the other tested mammals (Fig. 2d and Supplementary Fig. 5). We also found that the expression of nAChRs in somatotrophs of a Siberian tiger cub (Fig. 2e). These findings underscore the species-specific expression of nAChR subunits α3, β4, and α5 in the pituitary gland of Siberian tigers, both in early life and adulthood.

Functional nAChRs in Siberian tiger somatotrophs

The unusual expression of nAChR subunits in Siberian tigers prompted us to investigate the electrophysiological properties of the Siberian tiger nAChRs in the pituitary gland, specifically those formed by subunits α3, β4, and α5. Consistently, nAChRs are ligand-gated cation channels of the cys-loop superfamily[25]. In chick[26], mouse[27], and human[28], the subunits α3, β4, and α5 are sufficient to assemble into functional heteropentamers, either as α3β4 or α3β4α5. We constructed and coexpressed plasmids encoding α3, β4, and α5 of Siberian tiger nAChRs in human embryonic kidney 293 (HEK293) cells. Whole-cell recordings demonstrated that nAChRs α3β4 and α3β4α5 could be activated by acetylcholine at a holding potential of −70 mV (Fig. 3a, b and Supplementary Fig. 4). The half-maximal effective concentrations (EC_{50}) were 45.3 ± 1.2 μM and 65.8 ± 1.1 μM, respectively (Fig. 3c), which is similar to the acetylcholine sensitivity observed in other mammalian nAChRs[29,30]. Both α3β4 and α3β4α5 channels exhibited permeability to monovalent and divalent ions, including Na^+, K^+, and Ca^{2+} (Fig. 3d–g). Therefore, HEK293 cells expressing either α3β4 or α3β4α5 showed robust calcium signals at room temperature when activated by acetylcholine (Fig. 4a–c). These findings suggest that α3β4 and α3β4α5 in the Siberian tiger are functional calcium-permeable channels, which likely results in calcium signals in pituitary somatotrophs through their activation. Previous studies have demonstrated that elevated intracellular calcium ion concentrations in somatotrophs enhance GH secretion[14,31]. Therefore, these results prompted us to test whether the α3β4 or α3β4α5 channels are sufficient to regulate GH secretion in somatotrophs via nAChR activation at the cellular level.

Activation of nAChRs enhances growth hormone secretion

To evaluate the impact of nAChRs on GH secretion, we employed GH3 cells, a rat pituitary tumor cell line capable of secreting GH, to assess GH secretion in the presence or absence of α3β4 or α3β4α5 channels. Supernatants from GH3 cells treated with varying concentrations of acetylcholine were analyzed using an enzyme-linked immunosorbent assay (ELISA) to measure GH levels at 0, 10, 30, 60, 90, 120, and 180 min. As expected, GH secretion remained unchanged in GH3 cells, whether exposed to acetylcholine or not (Fig. 4d, e). Furthermore, GH secretion remained intact in GH3 cells transfected with α3β4 or α3β4α5 in the absence of acetylcholine. Notably, in the presence of 0.5 μM, 5 μM, and 50 μM acetylcholine, GH secretion began to increase at 10 min, reaching a maximum of 36.98% (± 2.13% s.e.m.) at 120 minutes in GH3 cells transfected with α3β4 or α3β4α5 (Fig. 4e), indicating an immediate and short-term response in GH regulation. Consistently, the nAChR inhibitor tubocurarine blocked the acetylcholine-mediated GH increase (Fig. 4d). These results suggest that nAChR activation facilitates calcium influx in the presence of acetylcholine, thereby enhancing GH secretion in GH3 cells. Together, our findings imply a nAChR-induced GH secretion mechanism in the pituitary somatotrophs of Siberian tigers.

Acetylcholine in mammalian pituitary glands

While the activation of nAChRs has been shown to promote GH secretion at the cellular level, the presence of sufficient acetylcholine in the pituitary gland of the Siberian tiger remains uncertain. Compared to the effective acetylcholine concentration (0.5 μM) required for GH release in cellular assays, we anticipated that the acetylcholine concentration needs to exceed 0.073 ng/mg to induce GH release, aligning with its critical role in other pituitary-regulated physiological processes[32,33]. To better understand the dynamics of acetylcholine levels (Supplementary Fig. 3) in the pituitary gland across different species, we examined its concentration in mice, rats, and domestic cats throughout their lifespan. Notably, we observed that acetylcholine levels were elevated during early life stages in these species (Fig. 5a–c), exceeding the minimum concentration (0.5 μM) required to activate nAChRs (Fig. 4e). This suggests that acetylcholine levels are likely sufficient to activate nAChRs during the early development of Siberian tigers. Moreover, acetylcholine content in the pituitary glands of these mammals declined with age. The average minimum acetylcholine concentrations in adult mice, domestic cats, rats, and Siberian tiger were 0.96 ng/mg (± 0.12, s.e.m.), 3.67 ng/mg (± 0.28, s.e.m.), 1.15 ng/mg (± 0.10, s.e.m.), and 0.35 ng/mg, respectively (Fig. 5a–d). Interestingly, the higher acetylcholine concentrations during early life coincided with periods of rapid growth, suggesting that the nAChRs expressed in the pituitary somatotrophs of the Siberian tiger might take advantage of these elevated acetylcholine levels to accelerate GH release during early development. The exceptionally large body size of Siberian tiger may be attributed to a unique GH release mechanism involving nAChRs expression in pituitary somatotrophs. During early development, acetylcholine activates these nAChRs, increasing Ca^{2+} influx and enhancing GH secretion, likely contributing to their substantial growth (Fig. 5e). Notably, nAChRs expression in somatotrophs persists into adulthood; however, pituitary acetylcholine levels decline significantly with age (~2.4 μM in adult Siberian tiger), suggesting that this mechanism is primarily active during early development and plays a limited role in post-maturational growth. Nevertheless, the persistent expression of nAChRs in adult Siberian tiger may still support the basal functionality of somatotrophs.

Discussion

Intracellular Ca^{2+} signaling is a well-established mediator of GH secretion in pituitary somatotrophs. Typically, growth hormone-releasing hormone receptor -liganded GHRH (growth hormone releasing hormone) stimulates somatotrophs, leading to an increase in cAMP, which in turn regulates calcium channels, elevating intracellular Ca^{2+} levels and thereby enhancing GH secretion[14,31]. The control of Ca^{2+}-mediated increase in GH secretion is largely dependent on Ca^{2+} influx in somatotrophs, because blocking calcium
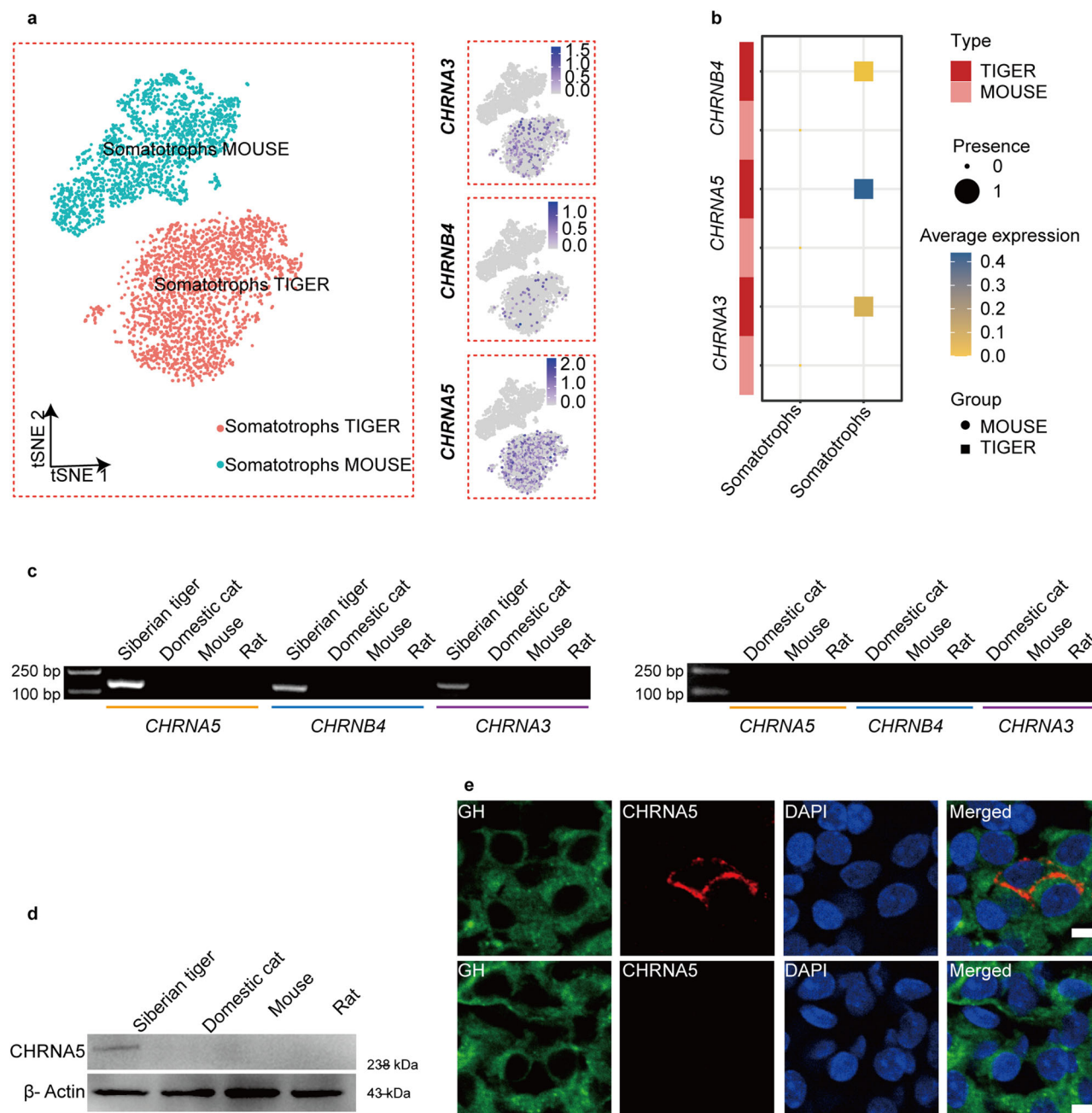
Fig. 2 | Species-specific expression of genes encoding nAChRs in the pituitary of Siberian tiger. a t-SNE plot showing somatotrophs atlas of Siberian tiger and mouse pituitary gland. Insert shows expression of *CHRNA3*, *CHRNB4*, and *CHRNA5* encoding nAChRs. **b** Comparison of *CHRNA3*, *CHRNB4*, and *CHRNA5* differential expression in somatotrophs between the Siberian tiger and the mouse. **c** Expression level of *CHRNA3*, *CHRNB4*, and *CHRNA5* genes in the pituitary gland is shown in the left panel for adult Siberian tiger (n = 1), domestic cat (n = 3), mouse (n = 6), and rat (n = 6), and in the right panel for juvenile domestic cat (n = 3), mouse (n = 6), and rat (n = 6). **d** Expression level of CHRNA5 protein in the pituitary gland of Siberian tiger (n = 1), domestic cat (n = 3), mouse (n = 6) and, rat (n = 6), assessed by Western blot on non-denaturing gels. **e** Representative immunofluorescence of GH and CHRNA5 (α5) in the pituitary of a Siberian tiger cub (top) and a mouse (bottom). The panels display confocal images of GH (green), α5 (red), DAPI-stained nuclei (blue), and merged images showing dual fluorescence labeling with DAPI. Scale bar: 10 μm.

channels or removing extracellular Ca^{2+} can reduce the release of GH[34,35]. Based on our findings, acetylcholine activated nAChRs in somatotrophs of Siberian tiger, likely providing an additional source of calcium signals in increasing GH. We suggest that while α3β4 and α3β4α5 play a critical role in regulating intracellular Ca^{2+} levels in pituitary somatotrophs, these nAChRs may work together as a physiological parallel with the typical signal to navigate the Siberian tiger to achieve rapid body growth (Fig. 5d).

Acetylcholine is known to function as both an autocrine and paracrine factor in the pituitary gland[36]. Its release, degradation, and biosynthesis have

been extensively studied across various mammalian pituitary glands[37], including the rat's anterior lobe[38,39], the rabbit's posterior lobe[40], and the pig's intermediate lobe[40,41]. Acetylcholine inhibits the corticotropin and prolactin release[32,38,42] while stimulating the secretion of α-MSH (alpha-melanocyte-stimulating hormone) from melanotrophs[33,43]. These studies suggest that the high expression of acetylcholine in the pituitary during early developmental stages may be involved in crucial, evolutionarily conserved biological processes in mammals, such as the modulation of the somatotropic, adrenocortical and prolactin axis[32,38,42]. Therefore, we hypothesize that the
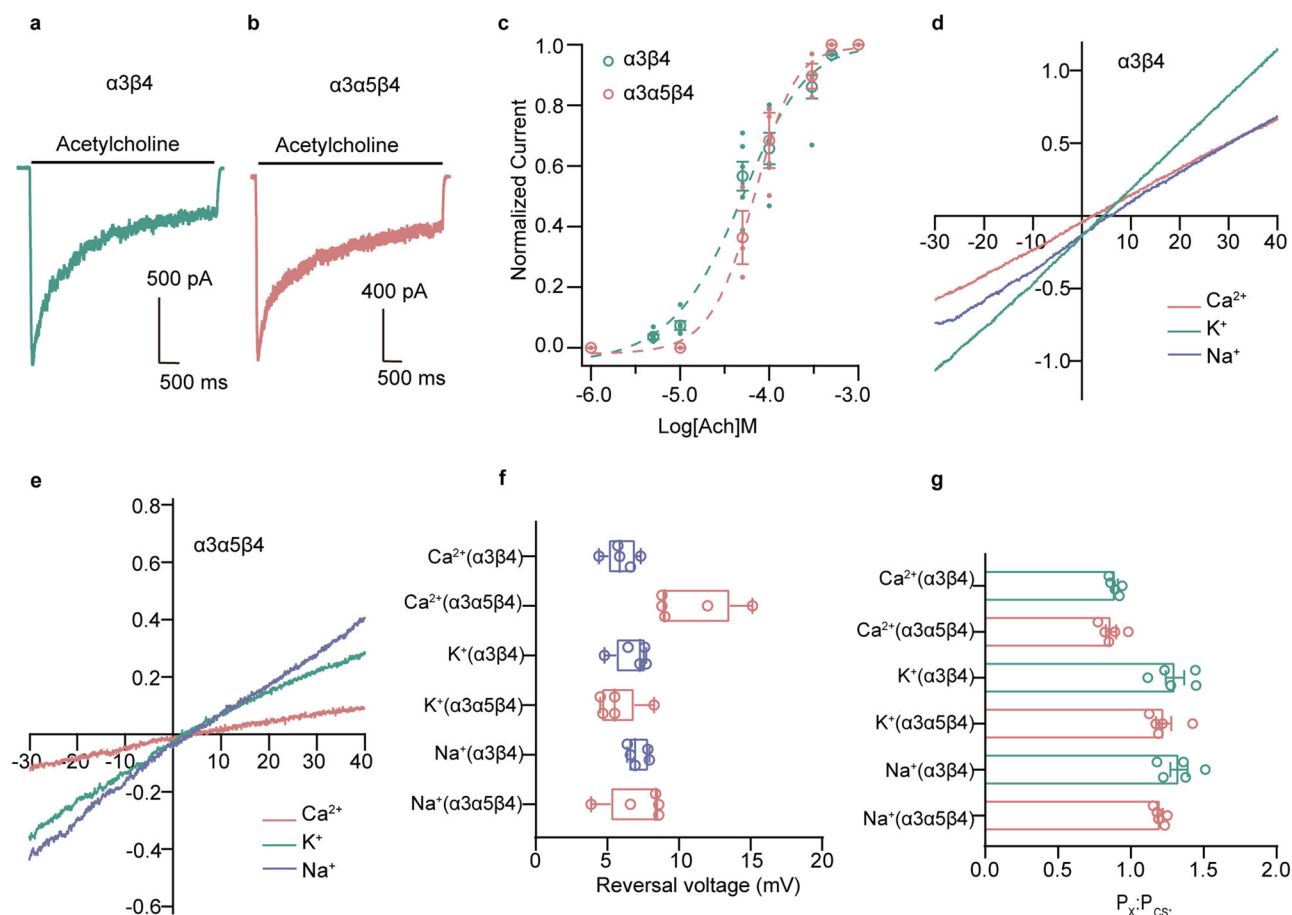
Fig. 3 | Activation of nAChRs in the Siberian tiger. a, b Whole cell currents of Siberian tiger α3β4 and α3β4α5 activated by 100 μM acetylcholine. All patches were recorded at a holding potential of −70 mV. **c** Concentration-response relationships of Siberian tiger α3β4 and α3β4α5 for acetylcholine fitted to a Hill equation (n = 5 per data point). All patches were recorded at a holding potential of −70 mV. **d, e** Current-voltage relationship of various cations for α3β4 and α3β4α5-transfected cells. **f** Reversal potentials of different cations for α3β4 and α3β4α5-transfected cells

(n = 5 cells for each group). α3β4 E_{rev} (Na$^+$ k$^+$ Ca^{2+}) = 6.4 ± 0.6 mV, 6.1 ± 0.9 mV, 5.4 ± 0.8 mV, respectively; α3β4α5 E_{rev} (Na$^+$ k$^+$ Ca^{2+}) = 6.6 ± 1.6 mV, 5.1 ± 1.2 mV, 9.8 ± 2.2 mV, respectively. **g** Ion permeabilities for α3β4 and α3β4α5 activated by acetylcholine (n = 5 cells per group). α3β4 (P_{Na}/P_{Cs} = 1.33; P_k/P_{Cs} = 1.30; P_{Ca}/P_{Cs} = 0.90); α3β4α5 (P_{Na}/P_{Cs} = 1.20; P_k/P_{Cs} = 1.23; P_{Ca}/P_{Cs} = 0.86). All statistical data are given as average ± SEM.

dynamics of acetylcholine in the Siberian tiger may be comparable to that of other mammals studied. It is widely accepted that the period of rapid growth in mammals typically occurs during the early stages of life[44]. Given our findings that acetylcholine reaches its highest levels during early mammalian life, it is possible that Siberian tigers utilize this shared mammalian characteristic for additional regulation of GH secretion by pituitary somatotrophs.

For mammals, various factors influence body size. At the ecological level, niche adaptation is a key driver of body size evolution, while environmental factors such as temperature and land area may limit maximum size[1,45]. Predator-prey dynamics also play a critical role; for instance, in blue whales, the spatial and temporal availability of prey constrains body size[46]. At the molecular level, body size is regulated by the growth hormone (GH) axis, which involves the secretion of GHRH by the hypothalamus to stimulate the pituitary gland[47], the binding of GH to its receptor (GHR) in target tissues[48], and the secretion of IGF-1 by the liver[49]. Although acetylcholine can stimulate GH secretion in the neonatal pituitary of mammals[50], our study proposes that the nAChR-mediated mechanism of Siberian tigers may serve as an additional pathway to enhance GH secretion by pituitary somatotrophs. Therefore, the complexity of these factors influencing body size also raises the question of whether the mechanism observed in the Siberian tiger also exists in other large terrestrial animals, or even in extinct large mammals. If so, future research should explore whether the pituitary somatotrophs of other large mammals exhibit high expression

of nAChRs into adulthood. Our findings not only enhance our understanding of body size regulation in large felids but also provide insights into the evolution and adaptation of large mammals.

Methods
Animals
All animal experiments adhered to the Guide for the Care and Use of Laboratory Animals of Northeast Forestry University and were approved by the Science and Technology Ethics Committee (approval No: 2024080). Efforts were made to minimize both sample size and animal suffering.

A 6-year-old Siberian tiger used in this study was obtained from the Siberian Tiger Park in Harbin, Heilongjiang. This tiger died due to injuries sustained in a fight. Domestic cats, sourced from the Feline Research Center of the National Forestry and Grassland Administration, were humanely euthanized via intravenous injection of an anesthetic overdose, ensuring rapid unconsciousness and cardiac arrest. Mice and rats were purchased from Liaoning Changsheng Biotechnology Co., Ltd. and euthanized using a graded CO_2 inhalation method. Briefly, the animals were placed in a chamber connected to a CO_2 gas cylinder, and the gas concentration was gradually increased to ensure rapid unconsciousness and subsequent death. All procedures adhered to ARRIVE guidelines and institutional ethical protocols to minimize pain and distress.

In this study, most data—PCR and Western blot (WB) analyses—were derived from the adult Siberian tiger that died in a fight. This represents an
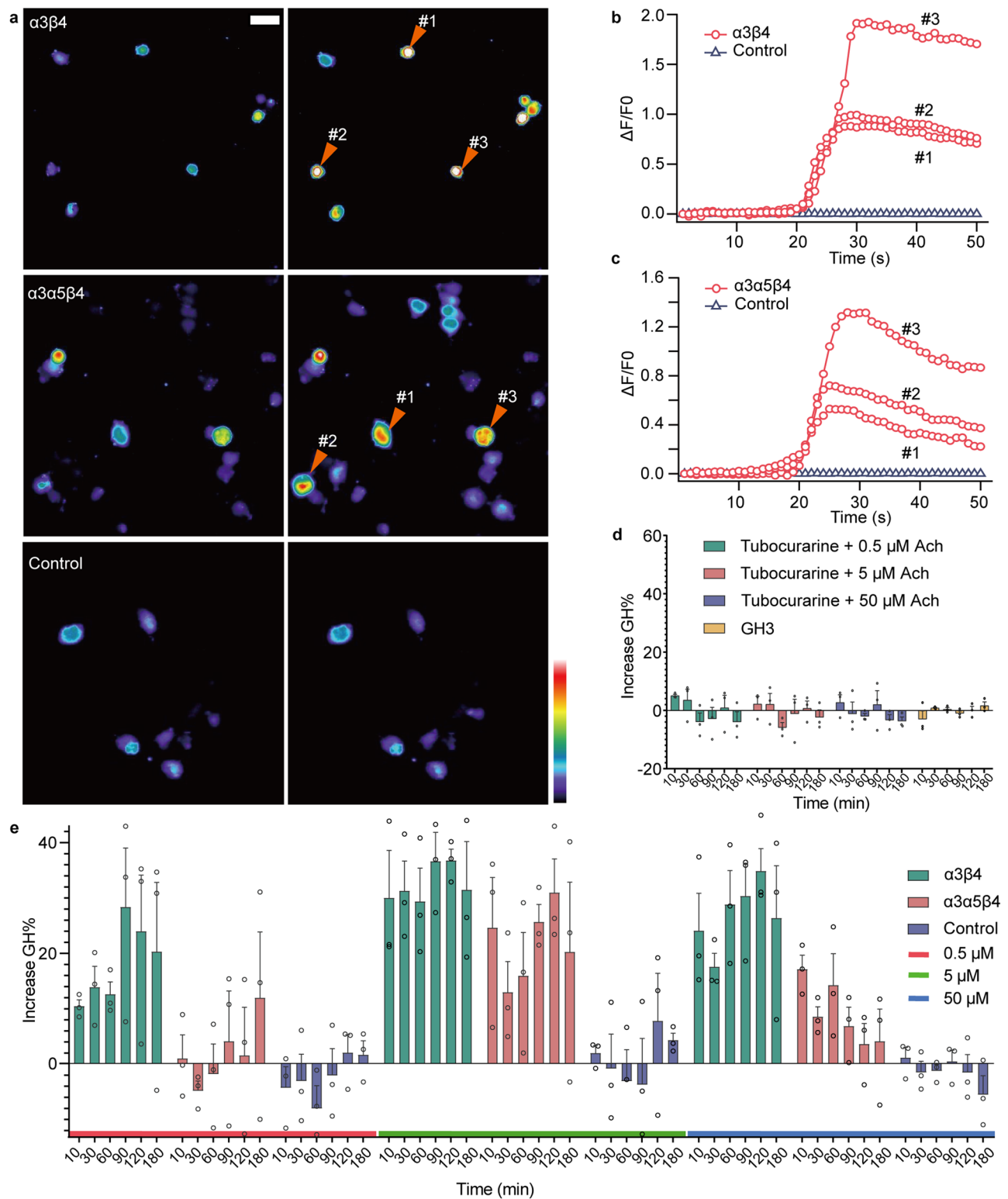
Fig. 4 | Calcium signals induced by acetylcholine and assay of growth hormone.
a Calcium fluorescence imaging of untransfected HEK293 cells and HEK293 cells expressing nAChRs α3β4 and α3β4α5. All cells before (left) and during (right) treatment with 100 μM acetylcholine. The color scale represents the calcium fluorescence intensity. Scale bar: 50 μm (horizontal), 1208–4089 a.u. (vertical). **b**, **c** Representative traces of calcium fluorescence signals were counted from nAChRs activation assays induced by acetylcholine. **d** ELISA assay of GH secretion at different times from GH3 cells transfected with α3β4 and α3β4α5 inhibited by various concentrations of tubocurarine and from untransfected GH3 cells in the absence of acetylcholine. (n = 3 for each independent experiment). **e** ELISA assay of GH secretion at different times from GH3 cells transfected with α3β4 and α3β4α5 activated by varying concentrations of acetylcholine (n = 3 for each independent experiment). All statistical data are given as average ± SEM.
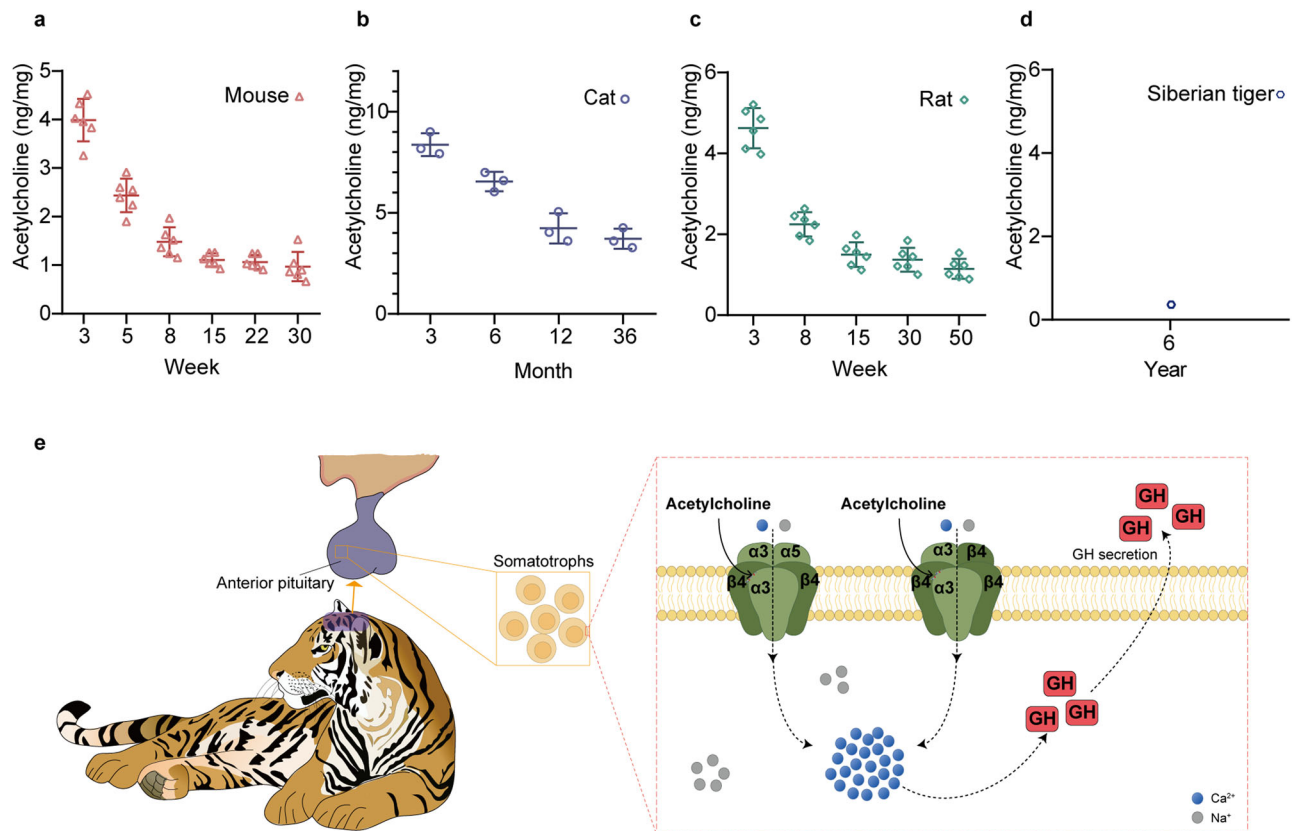
Fig. 5 | The necessary factors of nAChRs activated in somatotrophs of Siberian tiger. a–d Acetylcholine assay of mouse (3, 5, 8, 15, 22 and 30 weeks old), domestic cat (3, 6, 12 and 36 months old), rat (3, 8, 15, 30 and 50 weeks old) and Siberian tiger (6 years old) pituitary gland by UPLC-MS [domestic cat (n = 3), mouse (n = 6), rat (n = 6) and Siberian tiger (n = 1)]. The concentration of acetylcholine in the adult Siberian tiger pituitary is approximately 2.4 μM. **e** Schematic diagram of regulation hypothesized mechanism contributing to body size of Siberian tiger. All statistical data are given as average ± SEM.

adult developmental stage, comparable to six 12-week-old mice and rats (adult stage) and three 30-month-old domestic cats (young adult stage). Additionally, PCR analyses also included samples from six 3-week-old mice and rats (juvenile stage), and three 3-month-old domestic cats (juvenile stage). For the single-nucleus RNA sequencing and the acetylcholine concentration experiment, the Siberian tiger sample came from the same adult individual, while the comparison data were obtained from 10–12-week-old mice. Specifically, the pituitary gland of a Siberian tiger cub (5-month-old, sourced from the Feline Research Center of the National Forestry and Grassland Administration) was used for immunofluorescence.

Single nucleus RNA sequencing and assay
A Siberian tiger pituitary gland was dissociated into single-cell suspensions, and nuclei were subsequently isolated. After filtration, nuclei concentration (1080 nuclei/μl) was determined using a Countess II FL Automated Cell Counter. Library for sequencing was prepared using the 10x Genomics Chromium system with Chromium Next GEM Single Cell 3' Reagent Kits v3.1 (CG000204, 10x Genomics). Sequencing was performed on the NovaSeq 6000 platform (PN 20012850, Illumina). Raw sequencing data quality is shown in Supplementary Table 1.

Sn-RNA-seq data were processed using the Cell Ranger pipeline (version 6.1.2). The previously generated FASTQ sequencing data were mapped to the reference genome (GCF 018350195.1, NCBI), followed by cell and UMI counting to generate gene expression matrices using Cell Ranger count with default parameters. Single-cell analysis was then performed using Seurat (version 4.1.0) in R (version 4.2.1). This analysis included quality control, data normalization, variable gene identification, principal component analysis, dimensionality reduction, clustering, and visualization using the RunTSNE function, followed by manual annotation of clusters.

Mouse pituitary SnRNA-seq data obtained from NCBI (GSE151962) were analyzed similarly. The somatotrophs data from Siberian tiger and mouse were merged, and batch effects were removed using the Harmony package (version 0.1.1). Subsequent to grouping and visualization of the cell clusters, we conducted a differential gene expression analysis using the FindMarkers function (part of the Seurat package, version 4.1.0) in the R programming language (version 4.2.1) to compare gene expression profiles between Siberian tiger and mouse somatotrophs.

Cell culture and transient transfection
The cDNAs encoding Siberian tiger *CHRNA3* (XM 042987819), *CHENB4* (XM 042987648), and *CHRNA5* (XM 042987821), optimized for codon usage, were synthesized by Sangon Biotech (Shanghai, China) and subcloned into the pCDNA3.1 vector.

GH3 cells were obtained from the Cell Resource Center, Peking Union Medical College, and cultured in Ham's F-12 medium supplemented with 2.5% fetal bovine serum, 15% horse serum, and 1% penicillin/streptomycin. The cells were incubated at 37 °C in 5% CO_2 and transiently transfected with the channel-expressing plasmid using Lipofectamine 3000 transfection reagent (Life Technologies, USA), following the manufacturer's instructions. ELISA recordings were performed 24–48 h post-transfection.

HEK293 cells, purchased from the Kunming Cell Bank, Kunming Institute of Zoology, Chinese Academy of Sciences, were cultured in Dulbecco's modified Eagle's medium supplemented with 10% fetal bovine serum and 1% penicillin/streptomycin at 37 °C in 5% CO_2. These cells were transiently transfected with a mixture of the channel-expressing plasmid and a green fluorescent protein reporter plasmid using Lipofectamine 3000 transfection reagent. Calcium imaging and patch-clamp recordings were conducted 24 h post-transfection.

Electrophysiology

Whole-cell recordings were conducted at room temperature using an EPC10 amplifier and PatchMaster software (HEKA Elektronik, Germany). Patch pipettes were fabricated from borosilicate glass and fire-polished to a resistance of ~4 MΩ. For Siberian tiger pituitary gland nAChR channels (α3β4 and α3β4α5) recordings, a holding potential of −70 mV was applied. Transfected nAChR cells were positioned at the perfusion tube outlet, and varying concentrations of acetylcholine were delivered via a gravity-driven system (RSC-200, Biological Science Instruments) with nine separate tubes, while currents were recorded. The bath solution for whole-cell recordings contained: 140 mM NaCl, 5 mM KCl, 2 mM $CaCl_2$, 2 mM $MgCl_2$, 10 mM HEPES, 10 mM glucose (pH 7.4 adjusted with NaOH). The pipette solution contained: 112.5 mM K-aspartate, 20 mM KCl, 1 mM $MgCl_2$, 10 mM EGTA, 5 mM HEPES, 2 mM Mg adenosine triphosphate (pH 7.3 adjusted with KOH).

After establishing the whole-cell configuration in the bath solution, monovalent cation (Na^+ and K^+) substitution experiments were performed by replacing the bathing solution with 140 mM NaCl or KCl, 10 mM HEPES, and 10 mM glucose (pH 7.4 adjusted with NaCl or KCl, respectively). For divalent cation (Ca^{2+}) permeability experiments, the bathing solution was changed to 110 mM $CaCl_2$, 2 mM $Ca(OH)_2$, 10 mM HEPES, and 10 mM glucose (pH 7.4 adjusted with HCl). The pipette solution for ion substitution experiments contained 140 mM CsCl, 10 mM HEPES and 5 mM EGTA (pH 7.4 adjusted with CsOH). Voltage ramps (−40 to +100 mV in 500 ms) were applied to generate current–voltage curves in bath solutions with the indicated cation compositions and 100 μM acetylcholine. Permeability ratios for monovalent cations (P_X/P_{Cs}) were calculated as previously described[51]: $P_X/P_{Cs} = \exp(\Delta V_{rev} F/RT)$, where V_{rev} is the reversal potential, F is Faraday's constant, R is the universal gas constant, and T is absolute temperature. For measurements of divalent permeability, $P_Y/P_{Cs} = [Cs^+]_i \ \exp(\Delta V_{rev} F/RT)(1 + \exp(\Delta V_{rev} F/RT))/4[Y^{2+}]_o$, with assumed ion activity coefficients of 0.75 for monovalents and 0.25 for divalents.

Acetylcholine concentration

Pituitary glands were collected from C57BL/6 mice (3, 5, 8, 15, 22 and 30 weeks old), domestic cats (3, 6, 12 and 36 months old), SD rats (3, 8, 15, 30 and 50 weeks old) and Siberian tiger (5 years old). Upon collection, pituitaries were homogenized in precooled acetonitrile and methanol (1:1, v/v) and incubated on ice for 15 min. The homogenate was centrifuged at 12,000 rpm for 10 min, and the supernatant was collected. After volatilizing the supernatant, 200 μl acetonitrile was added, and the samples were prepared for analysis.

Acetylcholine levels were assessed using an Acquity™ Ultra Performance Liquid Chromatograph (UPLC, Waters, USA) coupled to a Triple TOF 6600 mass spectrometer (AB SCIEX, USA). The chromatography mobile phase B was 100% acetonitrile, while phase A was water. Initial conditions were set at 98% A, maintained for 1 min at a flow rate of 0.2 mL/min, followed by a linear gradient of solvent B increasing from 2% to 40% over 2 min. The system was then returned to its initial condition within 0.5 min and maintained for an additional 1.5 min. Mass spectrometry settings included a 5.5 kV ion spray voltage, a 500 °C ion source temperature, and precursor-to-product ion transitions established via direct infusion of acetylcholine standards into the ion source. Collision energy was set to 28 V, and the declustering potential was 60 V. Analysis was performed in positive ion mode, monitoring the m/z $146.1 \rightarrow 86.3$ transition for acetylcholine (Supplementary Fig. 3) using an external standard method.

Growth hormone secretion

GH3 cells, both non-transfected (control group) and transfected with α3β4 and α3β4α5, were evenly distributed across a 24-well plate, forming three experimental groups and the medium was changed to serum-free medium for 6 h. At 0 min, acetylcholine was added into 24-well plate and the concentrations of acetylcholine in plate of the three groups were 0.5 μM, 5 μM and 50 μM, respectively. GH levels in the supernatants were measured at 0,

10, 30, 60, 90, 120, and 180 minutes using rat enzyme-linked immunosorbent assay (ELISA) kits from Gersion Biotech (Beijing, China), following the manufacturer's instructions. The ELISA used in our study has a sensitivity with a minimum detection concentration of less than 0.1 ng/mL, and its limit of detection ranges from 0.1 ng/mL to 24 ng/mL.

Calcium imaging

HEK293 cells transfected with nAChRs were loaded with Fluo-4 AM in Hank's Balanced Salt Solution (HBSS; 137 mM NaCl, 0.4 mM Na_2HPO_4, 5.4 mM KCl, 5.6 mM glucose, 0.4Mm KH_2PO_4, 4.2 mM $NaHCO_3$, 1.3 mM $CaCl_2$, 0.6 mM $MgSO_4$, 0.5 mM $MgCl_2$, pH 7.2). Fluorescence images were acquired using an Olympus IX81 microscope equipped with a Hamamatsu R2 CCD camera, controlled by MetaFluor software (Molecular Devices). Fluo-4 was excited using an X-Cite 120LED light source (Lumen Dynamics) with a 500/20 nm excitation filter, and fluorescence emission was detected with a 535/30 nm emission filter. Calcium signals were induced by adding acetylcholine to the HBSS bathing solution. Images were acquired using automated routines in MetaMorph software (Molecular Devices) and analyzed with Igor Pro (WaveMetrics).

PCR analysis

Total RNA was isolated from pituitaries of Siberian tiger, mice, rats and domestic cats using TRIzol reagent (Invitrogen) and reverse transcribed with the FastKing gDNA Dispelling RT SuperMix Kit (KR118, TIANGEN Biotech, China). nAChR transcripts from the pituitaries of different species were amplified using a PCR system (T100, Bio-Rad, USA) under the following conditions: 94 °C for 5 min, followed by 35 cycles of 94 °C for 30 s, 60 °C for 30 s, and 72 °C for 30 s, with a final extension at 72 °C for 10 min, samples were then held at 4 °C. Primers (Supplementary Table 3) were synthesized by Sangon Biotech. After completing PCR, the products were subjected to 1% agarose gel electrophoresis, followed by imaging and observation using a gel documentation system.

Immunoblotting and immunofluorescence

Proteins from the pituitary glands of Siberian tiger (6 years old), mice (12 weeks old), rats (12 weeks old), and domestic cats (30 months old) were separated by 6% non-denaturing gel electrophoresis. The proteins were then electrotransferred onto polyvinylidene fluoride (PVDF) membranes (Immobilon) and blocked with 5% bovine serum albumin (BSA; 4240GR500, BioFroxx) for 3 h. The antibodies diluted with 5% BSA were dissolved in tris-buffered saline containing 0.1% Tween 20 [TBST; tris base (2.42 g/L), NaCl (8 g/L), and 0.1% Tween 20 (pH 7.6)]. The PVDF membranes were incubated overnight at 4 °C with the primary antibody, followed by three 15-min rinses with TBST. The membranes were then incubated with a secondary antibody for 1 h at room temperature, rinsed again with TBST, and then exposed to chemiluminescent reagents. Images were captured using a Tanon-5200Multi instrument (Tanon). The immunoblotting was performed using the following antibodies: mouse CHRNA5 antibody (1:2000, 66363-1-lg, ProteinTech), mouse β-actin antibody (1:1500, #44030, Signalway Antibody), which were used as the primary antibodies, and horseradish peroxidase–labeled anti-mouse (1:1500, #7076, Cell Signaling Technology) antibodies were used as secondary antibodies.

A frozen pituitary gland fragment from cub Siberian tiger (5-month-old), stored in liquid nitrogen, was thawed in a pre-cooled mixture of 4% PFA and absolute ethanol (1:3) at −80 °C for 1 h, then transferred to an ice box and placed on a shaker at 4 °C for an additional 3 h to complete thawing. The samples were then fixed in 4% PFA at 4 °C for 24 h. Dehydration was performed sequentially in 20% and 30% sucrose solutions at 4 °C for 1–2 days. The tissues were subsequently embedded in OCT and sectioned into 10 μm frozen slices. Primary antibodies against GH and CHRNA5 were incubated at 4 °C overnight. Secondary antibodies were incubated at 37 °C for 1 h, followed by DAPI nuclear staining and mounting. Finally, the sections were observed under a spinning disk confocal superresolution microscope (Olympus Corporation, Japan). The immunofluorescence was performed using the following antibodies: rabbit CHRNA5 antibody (1:200,

Article

13516-1-AP, ProteinTech), mouse GH antibody (1:200; sc-374266, Santa), which were used as the primary antibodies, and Goat Anti-Mouse IgG (H + L) (1:500; 115-545-003, Jackson) and Donkey Anti-Rabbit IgG (H + L) (1:500; 711-165-152, Jackson) were used as secondary antibodies. Additionally, the α5 antibody used in this study demonstrates high specificity, which has been validated in the hippocampus tissues of the experimental animals (Supplementary Fig. 5).

All other methods and reagents used are described in the Supplementary Information in Supplementary Table 4.

Statistics and reproducibility

Electrophysiological data were analyzed using Igor Pro (WaveMetrics) and Prism GraphPad (version 8.0.1). All the results are presented as mean ± SEM. Statistical significance was assessed using the Student's t test, with significance accepted at $P < 0.05$.

Concentration-response relationships between acetylcholine and nAChR were fitted by the Hill function.

$$\frac{I_x}{I_{\max}} = 1 - \frac{EC_{50}^n}{[x]^n + EC_{50}^n}$$

Where I_x represents the difference between the steady-state nAChRs channel current and the leaking current in the presence of concentration $[x]$; $[x]$ represents the concentration of acetylcholine; I_{max} represents the difference between the maximal current amplitude and the leaking current; EC_{50} represents the concentration of acetylcholine at which activation is half-maximal; n represents the Hill coefficient.

Reporting summary

Further information on research design is available in the Nature Portfolio Reporting Summary linked to this article.

Data availability

Single-nucleus RNA-seq data have been deposited in GEO (GSE277208). All numerical source data for graphs and charts have been deposited at Zenodo (https://doi.org/10.5281/zenodo.14886229)[52]. Uncropped blot and gel images are available in the supplemental information (Supplementary Fig. 6).

Code availability

All original code has been deposited at Zenodo (https://doi.org/10.5281/zenodo.13762242)[53]. Any additional information required to reanalyze the data reported in this paper is available from the Shiyu Chen (chenshiyu180236@163.com) upon request.

References

1. Smith, F. A. et al. The evolution of maximum body size of terrestrial mammals. *Science* **330**, 1216–1219 (2010).
2. Gonyea, W. J. Adaptive differences in the body proportions of large felids. *Acta Anatom.* **96**, 81–96 (1976).
3. Hin, V. & de Roos, A. M. Evolution of size-dependent intraspecific competition predicts body size scaling of metabolic rate. *Funct. Ecol.* **33**, 479–490 (2019).
4. Vermeij, G. J. Gigantism and its implications for the history of life. *PloS one* **11**, e0146092 (2016).
5. Benson, R. B., Frigot, R. A., Goswami, A., Andres, B. & Butler, R. J. Competition and constraint drove Cope's rule in the evolution of giant flying reptiles. *Nat. Commun.* **5**, (2014). 3567.
6. Lamberski N. Felidae. In: *Fowler's Zoo and Wild Animal Medicine, Volume 8* (eds Miller R. E., Fowler M. E.) (Saunders, W. B.2015).
7. Yachmennikova, A. et al. Data integration for the general-purpose scale of tiger cubs ontogenesis. *J. Biol. Bull. Rev.* **8**, 245–255 (2018).
8. Liu, Y. C. et al. Genome-wide evolutionary analysis of natural history and adaptation in the world's tigers. *Curr. Biol.* **28**, 3840–3849.e3846 (2018).
9. Langle, P. R., Rose, R. K. & Hamilton, M. J. Prionailurus rubiginosus (Carnivora: Felidae). *Mamm. Species* **51**, 155–162 (2019).
10. Mazák V. Panthera tigris. *Mammalian species*, 1–8 (1981).
11. Sunquist M., Sunquist F. *Wild Cats of the World* (University of Chicago Press, 2002).
12. Kopchick, J. J. & Andry, J. M. Growth hormone (GH), GH receptor, and signal transduction. *Mol. Genet. Metab.* **71**, 293–314 (2000).
13. Lu, M., Flanagan, J. U., Langley, R. J., Hay, M. P. & Perry, J. K. Targeting growth hormone function: strategies and therapeutic applications. *Signal Transduct. Target. Ther.* **4**, 3 (2019).
14. Vélez, E. J. & Unniappan, S. Comparative update on the neuroendocrine regulation of growth hormone in vertebrates. Front. Endocrinol. **11**, 614981 (2020).
15. Kargi, A. Y. & Merriam, G. R. Diagnosis and treatment of growth hormone deficiency in adults. *Nat. Rev. Endocrinol.* **9**, 335–345 (2013).
16. Mayo, K. E., Godfrey, P. A., Suhr, S. T., Kulik, D. J. & Rahal, J. O. Growth hormone-releasing hormone: synthesis and signaling. *Recent Prog. Horm. Res.* **50**, 35–73 (1995).
17. Devesa, J., Almengló, C. & Devesa, P. Multiple effects of growth hormone in the body: is it really the hormone for growth?. *Clin. Med. Insights Endocrinol. diabetes* **9**, 47–71 (2016).
18. Herrington, J. & Carter-Su, C. Signaling pathways activated by the growth hormone receptor. *Trends Endocrinol. Metab.* **12**, 252–257 (2001).
19. Mazziotti, G., Lania, A. G. & Canalis, E. Skeletal disorders associated with the growth hormone-insulin-like growth factor 1 axis. *Nat. Rev. Endocrinol.* **18**, 353–365 (2022).
20. Li, C. H. & Evans, H. M. The isolation of pituitary growth hormone. *Science* **99**, 183–184 (1944).
21. Ranke, M. B. & Wit, J. M. Growth hormone—past, present and future. *Nat. Rev. Endocrinol.* **14**, 285–300 (2018).
22. Ruf-Zamojski, F. et al. Single nucleus multi-omics regulatory landscape of the murine pituitary. *Nat. Commun.* **12**, (2021). 2677.
23. Yeung, C. -M., Chan, C. -B., Leung, P. -S. & Cheng, C. H. K. Cells of the anterior pituitary. *Int. J. Biochem. Cell Biol.* **38**, 1441–1449 (2006).
24. Ramirez-Latorre, J. et al. Functional contributions of alpha5 subunit to neuronal acetylcholine receptor channels. *Nature* **380**, 347–351 (1996).
25. Merino P. *Chemical Biology of Neurodegeneration: a Molecular Approach* (John Wiley & Sons, 2019).
26. Yu, C. R. & Role, L. W. Functional contribution of the alpha5 subunit to neuronal nicotinic channels expressed by chick sympathetic ganglion neurones. *J. Physiol.* **509**, 667–681 (1998).
27. Frahm, S. et al. Aversion to nicotine is regulated by the balanced activity of β4 and α5 nicotinic receptor subunits in the medial habenula. *Neuron* **70**, 522–535 (2011).
28. Wang, F. et al. Assembly of human neuronal nicotinic receptor α5 subunits with α3, β2, and β4 subunits*. *J. Biol. Chem.* **271**, 17656–17665 (1996).
29. George, A. A. et al. Function of human α3β4α5 nicotinic acetylcholine receptors is reduced by the α5(D398N) variant. *J. Biol. Chem.* **287**, 25151–25162 (2012).
30. Papke, R. L., Wecker, L. & Stitzel, J. A. Activation and inhibition of mouse muscle and neuronal nicotinic acetylcholine receptors expressed in Xenopus oocytes. *J. Pharmacol. Exp. Ther.* **333**, 501–518 (2010).
31. Steyn, F. J. et al. Adiponectin regulate growth hormone secretion via adiponectin receptor mediated Ca^{2+} signalling in rat somatotrophs in vitro. *J. Neuroendocrinol.* **21**, 698–704 (2009).
32. Carmeliet, P. & Denef, C. Synthesis and release of acetylcholine by normal and tumoral pituitary corticotrophs. *Endocrinology* **124**, 2218–2227 (1989).

33. Lamacz, M. et al. Acetylcholine stimulates alpha-melanocyte-stimulating hormone release from frog pituitary melanotrophs through activation of muscarinic and nicotinic receptors. *Endocrinology* **125**, 707–714 (1989).

34. Holl, R. W., Thorner, M. O. & Leong, D. A. Intracellular calcium concentration and growth hormone secretion in individual somatotropes: effects of growth hormone-releasing factor and somatostatin. *Endocrinology* **122**, 2927–2932 (1988).

35. Lussier, B. T., Wood, D. A., French, M. B., Moor, B. C. & Kraicer, J. Free intracellular Ca^{2+} concentration ([Ca^{2+}]i) and growth hormone release from purified rat somatotrophs. II. Somatostatin lowers [Ca^{2+}]i by inhibiting Ca^{2+} influx. *Endocrinology* **128**, 583–591 (1991).

36. Zemková, H. & Stojilkovic, S. S. Neurotransmitter receptors as signaling platforms in anterior pituitary cells. *Mol. Cell. Endocrinol.* **463**, 49–64 (2018).

37. Caffe, A. R. Architecture of the mammalian pituitary cholinergic system with observations on a putative blood acetylcholine sensor. *Histol. Histopathol.* **11**, 537–551 (1996).

38. Carmeliet, P. & Denef, C. Immunocytochemical and pharmacological evidence for an intrinsic cholinomimetic system modulating prolactin and growth hormone release in rat pituitary. *Endocrinology* **123**, 1128–1139 (1988).

39. Gregg, C. M. The compartmentalized hypothalamo-neurohypophysial system: evidence for a neurohypophysial action of acetylcholine on vasopressin release. *Neuroendocrinology* **40**, 423–429 (1985).

40. Bridges, T. E., Fisher, A. W., Gosbee, J. L., Lederis, K. & Santolaya, R. C. Acetylcholine and cholinesterases (assays and light- and electron microscopial histochemistry) in different parts of the pituitary of rat, rabbit and domestic pig. *Z. Zellforsch. Mikrosk. Anat.* **136**, 1–18 (1973).

41. Tandon, A., Collier, B., Zhang, Z. W. & Feltz, P. Acetylcholine synthesis in a primary culture of porcine intermediate lobe cells. *J. Neuroendocrinol.* **3**, 273–277 (1991).

42. Rudnick, M. S. & Dannies, P. S. Muscarinic inhibition of prolactin production in cultures of rat pituitary cells. *Biochem. Biophys. Res. Commun.* **101**, 689–696 (1981).

43. van Strien, F. J., Jenks, B. G., Vaudry, H. & Roubos, E. W. Cholinergic regulation of the pituitary: autoexcitatory control by acetylcholine of melanotrope cell activity in Xenopus laevis. *Ann. N.Y. Acad. Sci.* **839**, 66–73 (1998).

44. Lui, J. C. & Baron, J. Mechanisms limiting body growth in mammals. *Endocr. Rev.* **32**, 422–440 (2011).

45. Baker, J., Meade, A., Pagel, M. & Venditti, C. Adaptive evolution toward larger size in mammals. *Proc. Natl. Acad. Sci. USA* **112**, 5093–5098 (2015).

46. Goldbogen, J. A. et al. Why whales are big but not bigger: Physiological drivers and ecological limits in the age of ocean giants. *Science* **366**, 1367–1372 (2019).

47. Lee, L. T. et al. Discovery of growth hormone-releasing hormones and receptors in nonmammalian vertebrates. *Proc. Natl. Acad. Sci. USA* **104**, 2133–2138 (2007).

48. da Silva Almeida, A. C., Strous, G. J. & van Rossum, A. G. βTrCP controls GH receptor degradation via two different motifs. *Mol. Endocrinol.* **26**, 165–177 (2012).

49. Brooks, A. J. & Waters, M. J. The growth hormone receptor: mechanism of activation and clinical implications. *Nat. Rev. Endocrinol.* **6**, 515–525 (2010).

50. Pintér, I., Makara, G. B. & Acs, Z. Acetylcholine stimulates growth hormone secretion in the neonatal rat pituitary. *J. Neuroendocrinol.* **8**, 935–939 (1996).

51. Caterina, M. J. et al. The capsaicin receptor: a heat-activated ion channel in the pain pathway. *Nature* **389**, 816–824 (1997).

52. Liu, L., Yang, S., & Chen, S. Numerical source data for graphs and charts-nicotinic acetylcholine receptors regulate growth hormone in pituitary somatotrophs of tigers [Data set]. *Zenodo* https://doi.org/10.5281/zenodo.14886229 (2025).

53. Liu, L., Yang, S., & Chen, S. R. Code-nicotinic acetylcholine receptors regulate growth hormone in pituitary somatotrophs of tigers. *Zenodo* https://doi.org/10.5281/zenodo.13762242 (2024).

Acknowledgements

Author contributions

Conceptualization, B.L., G.J., and S.C.; methodology, L.L., S.Y., and B.L.; investigation, L.L., S.Y., S.Z., H.X., Y.Z., and D.L.; formal analysis, L.L., S.Y., S.Z., L.C., S.C., G.J., and B.L.; resources, S.Y. and L.C.; writing—original draft, L.L., S.Y., S.C., G.J., and B.L.; writing—review & editing, S.Y., L.L., S.C., G.J., and B.L.; supervision, S.C., G.J., and B.L.

Competing interests

The authors declare no competing interests.

Additional information

Supplementary information The online version contains supplementary material available at https://doi.org/10.1038/s42003-025-07980-6.

Correspondence and requests for materials should be addressed to Shiyu Chen, Guangshun Jiang or Bin Li.

Peer review information *Communications Biology* thanks Yuhua Tian and the other, anonymous, reviewer for their contribution to the peer review of this work. Primary Handling Editor: Benjamin Bessieres. A peer review file is available.

Reprints and permissions information is available at http://www.nature.com/reprints

Publisher's note Springer Nature remains neutral with regard to jurisdictional claims in published maps and institutional affiliations.